J Electr Eng Technol.2017; 12(4): 1449-1455
http://doi.org/10.5370/JEET.2017.12.4.1449

ISSN(Print) 1975-0102
ISSN(Online) 2093-7423

Simple Bump-removal Scheme for the Position Signal of PM Motor Drives with Low-resolution Hall-effect Sensors

Dong-Myung Lee†

Abstract – The vector control technique using low-resolution Hall-effect sensors has been widely used especially in consumer electronics. Due to electrical and/or mechanical unevenness related to binary-type Hall sensors, the calculated or estimated position information has discontinuities so called bumps, which causes the deterioration of vector control performance. In order to obtain a linearly changing position signal from low-precision Hall-effect sensors, this paper proposes a simple bumps in position signal removal algorithm that consists of a first-order observer with low-pass filtering scheme. The proposed algorithm has the feature of no needs for system parameters and additional estimation processes. The validity of the proposed method is verified through simulation and experimental results.

Keywords: Position estimation, Bump-removal scheme, Hall-effect sensors, 1st order observer

1. Introduction

Permanent magnet synchronous motors (PMSMs), which have superior efficiency compared to other types of electric motors, are mainly used for washing machines [1]. The vector control scheme has been widely applied in home appliances to improve the control performance. The driving system of PMSMs employing a vector controller requires accurate rotor position information [2]. For a typical variable speed application, a highly accurate sensor, such as an encoder or resolver, is employed. However, since cost is an important factor for consumer products, binary-type Hall sensors, which generate square-wave signals corresponding to the N and S poles of the rotor, are commonly employed for position sensing, achieving proper control performance in an efficient way [3].

Various studies for obtaining high-resolution position information from binary-type Hall sensors have been conducted [4-12]. Some papers have suggested estimation methods based on the zeroth-order Taylor algorithm [4-6]. This method, which obtains the rotor position by using the integral of the average speed, is simple and easily gets the location information, but the accuracy of the mean velocity has a vulnerability resulting from mechanical misalignment and/or non-uniformity in the sensor circuits.

In [7], the angular velocity information was used to estimate the rotor position. However, in practice, it is difficult to obtain accurate acceleration information. In order to limit the amount of error in the estimation at low-speed operation, a position estimation method based on back-EMF has been proposed [8]. On the other hand, the precision of the detection depends on the accuracy in the motor parameters such as a stator resistance.

† Corresponding Author: School of Electronic and Electrical Engineering, Hongik University, Seoul, Korea. (dmlee@hongik.ac.kr)
Received: June 17, 2016; Accepted: December 12, 2016

Position estimation schemes using an observer have been presented in many researches [9-12]. The observer-based scheme is characterized by good dynamics and high estimation accuracy. However, the equations of observers are based on mechanical models of the system, and the mechanical model requires information about the load torque and the generated motor torque. Therefore, if there are inaccuracies in the values of mechanical parameters and miscalculation of the generated motor torque, the performance deterioration of the observer can not be avoided.

This research is about the performance improvement scheme in position detection for a washing machine. On the other hand, the normal working condition of a washing machine may not be ideal to apply a Luenberger position observer, since the conventional observer schemes require mechanical parameters and the calculation of motor torque in which uncertainty of the motor parameters may exist. In addition, the load torque and system parameters such as inertia of the washing machine are not fixed values, but change according to the amounts of water and laundry. The accuracy of position estimation highly depends on how well the method estimates system parameters. Thus, an additional algorithm is required for estimating the mechanical parameters and the motor torque, which increases the calculation burden of the controller [13]. In addition, the order of the conventional observer is 3rd.

To solve these problems, this paper proposes a new position detection scheme featuring a very simple structure, which obtains linearly changing position information from low-resolution Hall sensors without employing system parameters. The proposed scheme does not require calculation of either the motor torque or the load torque. The effectiveness of the proposed method is verified by simulation and experimental results carried out with a 48-pole permanent magnet synchronous motor.

It should be mentioned that the application of the proposed algorithm is not limited to Hall sensors. In [14], the position waveforms of a magnetic levitation train (Maglev) are shown, and their shape is similar to the position signals obtained from binary-type Hall sensors, and it is also noted that an algorithm for obtaining linearly changing position signal is necessary. Therefore, various applications exist, which require high-resolution position signal from low-precision sensors, for which the proposed algorithm can be applied.

2. Position Detection by Conventional Methods and Their Detected Position Signals

If two binary-type Hall sensors, which generate a 1 or 0 level corresponding to the polarity of the magnet, are installed in a 2π electrical span, the electrical resolution is $\pi/2$ radians. Thus, the electrical angular speed can be calculated as (1) by dividing $\pi/2$ by the time interval between Hall events (ΔT_{hall}) and the electrical angle at the nT sampling time can be calculated by the extrapolation expressed in (2).

$$\omega_{e\_cal}(nT) = (\pi/2)/\Delta T_{hall}(nT) \tag{1}$$

$$\theta_{e\_hall}(nT) = \theta_{e\_hall}[(n-1)T] + \omega_{e\_cal}(nT)\cdot T \tag{2}$$

Fig. 1 depicts Hall A & B signals, which have some angle discrepancies denoted as α, β, and γ from the ideal $\pi/2\cdot n$ (n=0,1,2, or 3) position, and their corresponding position waveforms. The term $\pi/2$ in the numerator of (1) is for the ideal case, i.e. the electrical span between the Hall sensor events is exactly $\pi/2$ radians. In general, the angle between Hall sensor events is not exact $\pi/2$ radians due to various causes such as unevenness in electrical circuits related to Hall sensors, inequality in mechanical installation, and non-uniformity in the flux of magnets in the rotor.

Under ideal conditions, the position information using (2) increases linearly without a bump in the position signal as shown by the dotted line. Position ① line illustrates $\theta_{e\_hall}(nT)$ obtained by (2). $\theta_{e\_hall}(nT)$ is updated as a multiple of $\pi/2$, which is depicted as position ②, with respect to the rising and falling Hall events. Hence, in practice, even at a constant speed operation, the difference in ΔT_{hall} generates the bumps in the position ① signal unlike the ideal case.

If the amount of angle deviation in the Hall events is fixed and is known in advance, the discontinuity in position ① signal can be removed by adding the predetermined values. However, in this research, the motor with multiple poles that have non-uniformity in flux-linkage with a non-iterative pattern is used so that the position calibration scheme of adding predetermined values is not applicable.

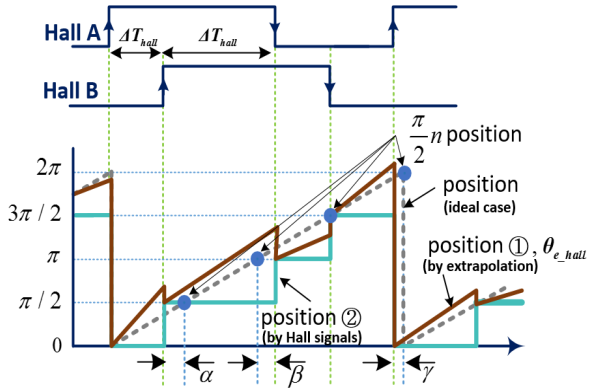

Fig. 1. Hall sensor signals and their associated position signals

The position detection by an observer is known to have excellent dynamic characteristics. However, there are some concerns. The state equation of the conventional observer is expressed as (3) - (5) with the assumption of slow load change during the sampling period T. As seen from (3) - (5), the observer method is based on the mechanical motion equation modeled with system information such as J and T_e [14]. (3) - (5) have the form of (6). Y means the measured value, θ_{e_hall}.

$$\frac{d\hat{\theta}_e}{dt} = \hat{\omega}_e + h_1\left(\theta_{e\_hall} - \hat{\theta}_e\right) \tag{3}$$

$$\frac{d\hat{\omega}_e}{dt} = \frac{1}{J}\frac{P}{2}\left(T_e - \hat{T}_L\right) + h_2\left(\theta_{e\_hall} - \hat{\theta}_e\right) \tag{4}$$

$$\frac{d\hat{T}_L}{dt} = h_3\left(\theta_{e\_hall} - \hat{\theta}_e\right) \tag{5}$$

where, T_L, T_e, θ_e, ω_e, h, J, and P represent load torque, developed motor torque, rotor electrical position, rotor angular frequency, observer gain, system inertia, and number of poles, respectively.

$$\begin{aligned} &\frac{d}{dt}\hat{X} = A\hat{X} + BU + H(Y - C\hat{X}) \\ &X^T = [\theta_e\ \omega_e\ T_L],\ Y = \theta_{e\_hall},\ C = [1\ 0\ 0] \end{aligned} \tag{6}$$

(3)-(5) show that ultimately to get the estimated θ_e of (3), the estimated ω_e by (4) is necessary, and for the ω_e calculation T_L estimation through (5) as well as the T_e calculation are required. The T_e of a SPM (surface-mounted permanent magnet) motor is given as $(3/2)\cdot(P/2)\cdot\lambda_a\cdot i_q$. Where, λ_a means the flux-linkage by a magnet, and i_q is q-axis current. Since λ_a, which varies with ambient temperature, is involved in the T_e calculation, it may lead to errors in the θ_e observation if there is no on-line λ_a estimation. Furthermore, observer gains of h_1–h_3 need to be set.

3. Proposed Bump-removal Scheme

To reduce the order of the observer as well as to remove the involvement of J and T_e in the position estimation procedure, a scheme based only on (3) is proposed in this paper. Since (4) and (5) are used to determine or estimate ω_e for the conventional observer, the proposed scheme is devised to get the estimated motor speed ($\hat{\omega}_e$, equivalently ω_{e_est}) through a low-pass filter (LPF). The state equation of the proposed observer is written as (7), and k represents the observer gain.

$$\frac{d\theta_{e\_est}}{dt} = \omega_{e\_est} + k\left(\theta_{e\_in} - \theta_{e\_est}\right) \tag{7}$$

The transfer function of the observer of (7) appears as (8). (8) remarks that the observer is a stable system when $k > 0$. The position input (θ_{e_in}) is obtained form (9). In (9), ω_{e_est}, which is the output of the LPF and the equivalent variable for $\hat{\omega}_e$ in (4), is used instead of ω_{e_cal}. Similarly to $\theta_{e\_hall}(nT)$, $\theta_{e\_in}(nT)$ is changed to $\pi/2 \cdot n$ radians corresponding to the rising and falling events of the Hall signals. Hence, the shape of θ_{e_in} is almost identical to θ_{e_hall}, but to have further bump-less transition in the rotor position, ω_{e_est} is employed for the θ_{e_in} calculation.

$$\theta_{e\_est}(s) = \frac{k}{s+k}\theta_{e\_in}(s) + \frac{1}{s+k}\omega_{e\_est}(s) \tag{8}$$

$$\theta_{e\_in}(nT) = \theta_{e\_in}[(n-1)T] + \omega_{e\_est}(nT)\cdot T \tag{9}$$

Fig. 2 illustrates the block diagram of the proposed method that removes bumps in the detected position signal in the absence of J and T_e terms. The proposed scheme consists of the first order observer and the low-pass filter that obtains ω_{e_est} from ω_{e_cal}. Where, $Tz^{-1}/(1-z^{-1})$ denotes the integration ($1/s$) in the discrete domain. To get a simpler form, the first-order LPF is used and the transfer function can be expressed as (10). Where, a represents the cut-off angular frequency ($2\pi f_c$), and f_c is the cutoff-frequency of the LPF.

$$Y(s) = \frac{a}{s+a}X(s) \tag{10}$$

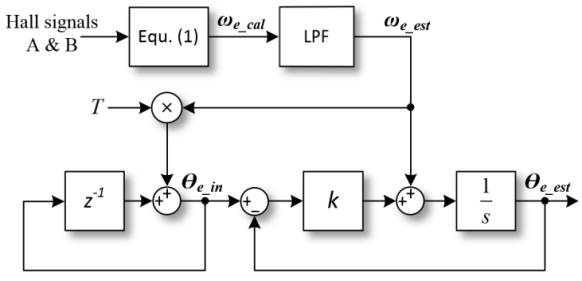

Fig. 2. Block diagram of the proposed bump-removal scheme

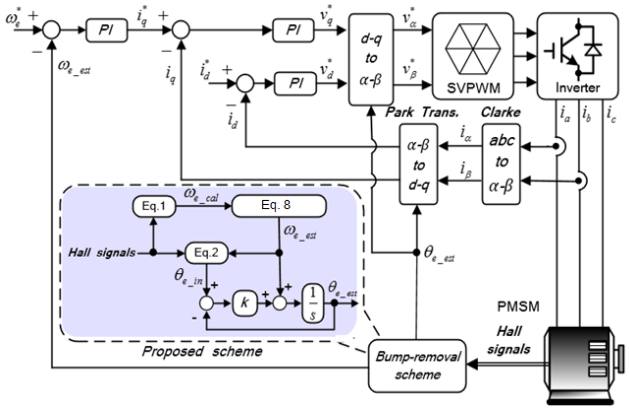

Fig. 3. Block diagram of the PM motor drive with the proposed scheme

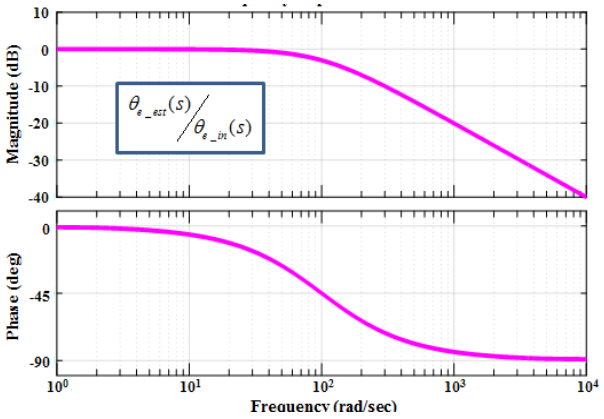

Fig. 4. Frequency response of the first term in (6) with the observer gain k=100

The expression of ω_{e_est} from the LPF in the discrete form can be given as (11). From (7), (9), (11), and Fig. 2, it is obvious that the proposed algorithm features a very simple structure and less calculation.

$$\omega_{e\_est}(nT) = m_1 \cdot \omega_{e\_est}[(n-1)T] + m_2 \cdot \omega_{e\_cal}(nT) \tag{11}$$

where, $m_1 = \tau / (\tau + T)$, $m_2 = T / (\tau + T)$, and $\tau = 1/f_c$.

Fig. 3 depicts an overall block diagram of the proposed method for vector control of the washing machine using low-resolution Hall sensors.

The Estimation block derives ω_{e_est} and the bump-less θ_{e_est} position through (11), and (7), respectively, and θ_{e_est} is fed to the axis-transformation block. The basic control technique of SPM motors is applied. In other words, in the constant torque area, i^*_d is chosen as 0 ampere, and field weakening control is used in the constant power region.

Fig. 4 illustrates the frequency response corresponding to the first term of (8). That is the frequency response of $\theta_{e\_est}(s)/\theta_{e\_in}(s)$. The figure shows that the phase delay at 100 rad/sec corresponding to the observer gain k=100 is 45^0.

4. Verifications

4.1 Simulation results of the proposed bump-elimination scheme

Fig. 5 is the simulation block diagram, implemented with MATLAB/Simulink, of the proposed algorithm shown in Fig. 2. In Block ①, Hall signals having non–uniformity in the interval are generated in accordance with the rotor's electrical angle. ω_{e_cal} and θ_{e_in} are calculated in Block ② by (1) and (7), respectively. Fig. 6 shows inside of Block ③. The term $k(\theta_{e\_in}–\theta_{e\_est})$ is used in Fig. 2 and 3. Meanwhile, in the actual implementation, the error between the angles is calculated by not $k(\theta_{e\_in}–\theta_{e\_est})$ but by $k\cdot\sin(\theta_{e\_in}–\theta_{e\_est})$ as shown in Fig. 6. Since, $\sin(\alpha\pm 2\pi)=\sin(\alpha)\approx\alpha$ for small α, taking the sine of $\theta_{e\_in}–\theta_{e\_est}$ inhibits the error caused by the additional $+2\pi$ or $–2\pi$ radians in the $\theta_{in}–\theta_{est}$ value occurring at the $2\pi\rightarrow 0$ or $0\rightarrow 2\pi$ transition. The LPF is implemented in Block ④. The specification of the SPM motor used for verifications is summarized in Table 1. Fig. 7 and 8 illustrate simulation results of the proposed scheme with k=100 performed with a 48-pole PMSM at 400 rpm operation. Upper figures depict ω_{e_cal} by (1) and ω_{e_est} from the LPF.

Table 1. Specification of the SPM motor used for verifycations

R_s	4.5 Ω	L_s	32 mH
λ_m	0.15 Wb	J	0.25 kg-m^2
No. of poles	48	Rated power	1 kW

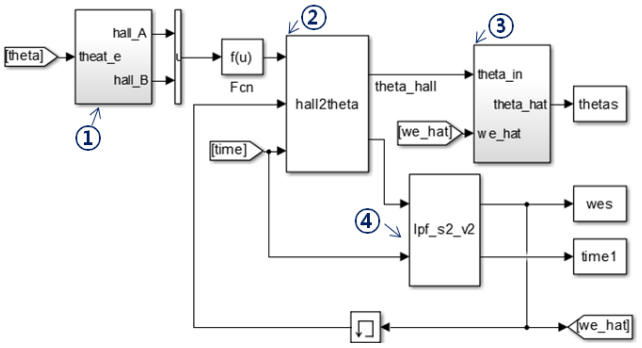

Fig. 5. Simulation block diagram for removing bumps in the position signal

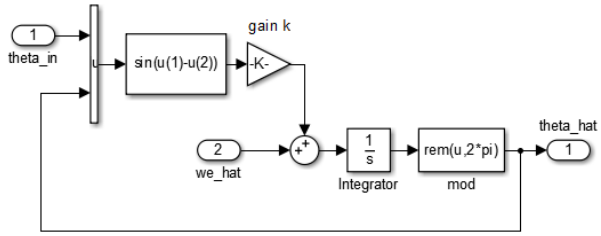

Fig. 6. Simulation block diagram of the internal working of Block ③ for implementing the observer part

The lower figures show the estimated rotor position (θ_{e_est}), θ_{e_in}, and Hall A & B signals that have about 4^0 larger or smaller angle interval compared to the ideal case. The cutoff-frequency (f_c) of the LPF for Figs. 7 and 8 has been selected with two cases- 80 Hz and 250 Hz. θ_{e_est} is located 1 radian above θ_{e_in} to discriminate two waveforms. Figs. 7 and 8 clearly display that the proposed scheme with k=100 and the LPF having 80 Hz or 250 Hz obtains bump-free θ_{e_est} from θ_{e_in} without angle discrepancy between θ_{e_in} and θ_{e_est}.

Considering the first term of (8), which is $k/(s+k)$, the –3 dB frequency with respect to k=100 is 15.92 Hz, and it corresponds to 39.79 rpm for a 48-pole machine. As this rpm is a way below 400 rpm, this observer gain (k=100) does not seem appropriate one for 400 rpm operation. Moreover, the phase response of θ_{e_est} against θ_{e_in} corresponding to the first term of (7) is calculated as 1.47 radians (84.32^0) at 400 rpm (f_e=160 Hz) operation with k=100. Therefore, almost $\pi/2$ lag is expected, but the angle delay of θ_{e_est} against θ_{e_in} is not observed in Figs. 7 and 8.

The reason for this can be explained as follows. For the ideal case, the interval between Hall signals accurately maintains $\pi/2$ radians so that ω_e can be given as $d\theta_e/dt$ since θ_e has no discontinuities. In this case, $\omega_e(s)$ can be represented as $\omega_e(s)=s\theta_e(s)$. In the proposed scheme, ω_{e_est} is the filtered ω_{e_cal}, so that ω_{e_est} can be roughly considered as $d\theta_e/dt$. In other words, $\omega_{e\_est}(s)\cong s\theta_e(s)$. Therefore, applying this relationship to (8) and manipulating that as shown in (12), it can be seen that θ_{e_est} coincides θ_{e_in} by utilizing filtered ω_{e_cal}.

$$\begin{aligned}\theta_{e\_est}(s)&=\frac{k}{s+k}\theta_{e\_in}(s)+\frac{1}{s+k}\omega_{e\_est}(s)\\&\approx\frac{k}{s+k}\theta_{e\_in}(s)+\frac{1}{s+k}s\theta_{e\_in}(s)=\theta_{e\_in}(s)\end{aligned}\tag{12}$$

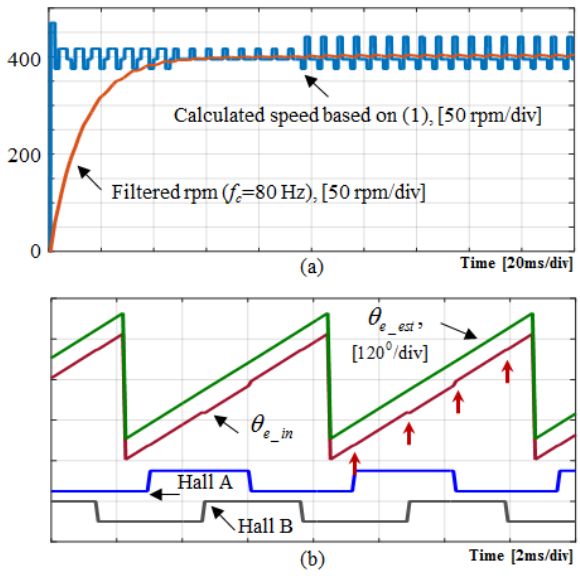

Fig. 7. Simulation results with k=100 and f_c=80 Hz

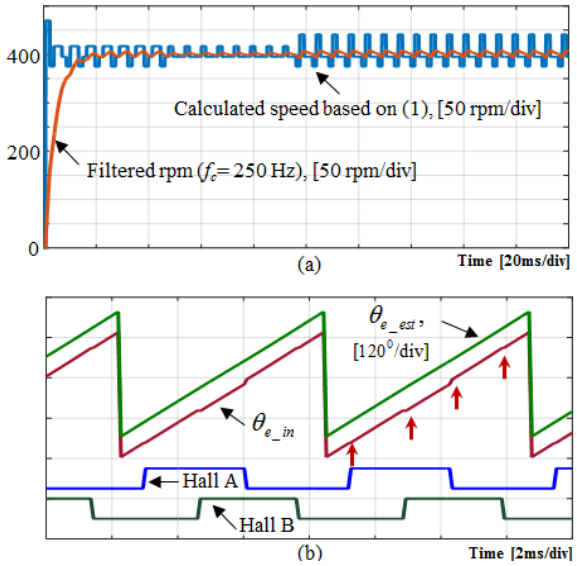

Fig. 8. Simulation results with k=100 and f_c=250 Hz

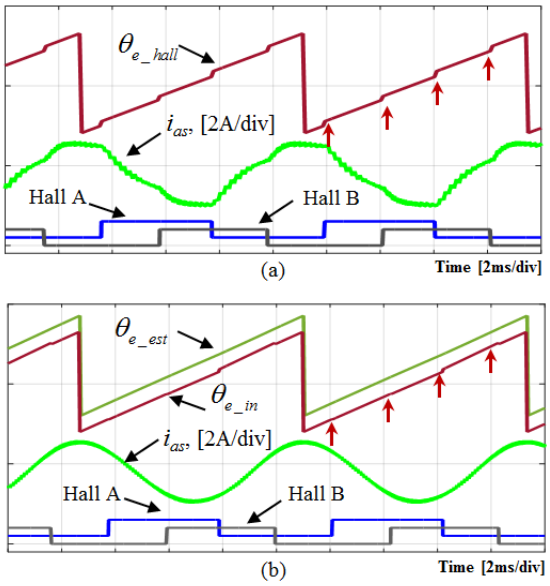

Fig. 9. Simulation results (a) without and (b) with the proposed bump-removal scheme at 300 rpm rotation with f_c=80 Hz, k=100, and 5 Nm load condition

As can be appreciated from the second line of (12), s+k terms are presented in both the numerator and denominator and are discarded in the last equation. Hence, the estimation capability according to the k value is not sensitive.

In addition, the estimated positions of Figs. 7 and 8 show the same bump-elimination performance even for different f_c of 80 or 250 Hz, which implies that the proposed scheme is relatively insensitive to f_c of the LPF, since the low-pass filtering makes the relationship of $\omega_{e\_est}(s) \cong s\theta_e(s)$ with different f_c values, having appropriate filtering effect. On the other hand, the positions of the bumps in Fig. 7 and that in Fig. 1 are different each other. In the experimental setup with a top-load washer, the Hall

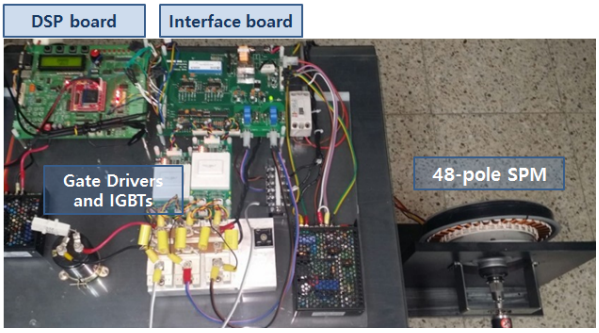

Fig. 10. Experimental setup

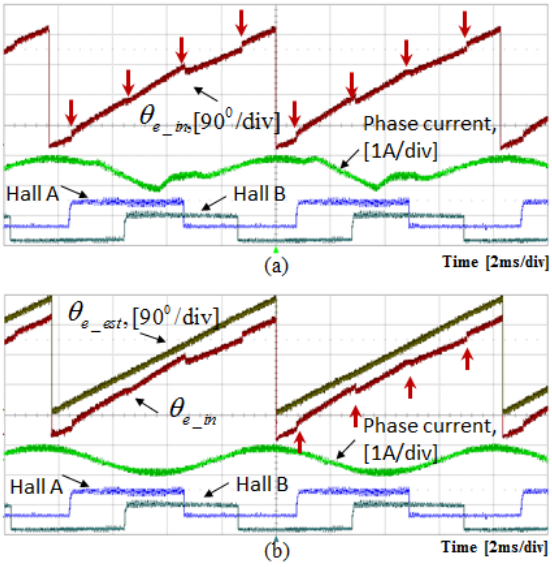

Fig. 11. Experimental waveform of position signals and phase current: (a) without the proposed scheme and (b) with the proposed bump-elimination scheme with k=150 and f_c=100 Hz

A sensor was installed to have the first signal occurrence at π/6 radians. Hence, this fact is reflected in the simulation studies. Fig. 9 shows the simulation waveforms at 300 rpm operation (a) without and (b) with the proposed method. The load condition is 5 Nm. As appeared in Fig. 9(a), bumps occur in θ_{e_hall} and resultant distorted current waveform. Fig. 9(b) clearly illustrates the linearly changing position signal of θ_{e_est} and sinusoidal phase current waveforms.

4.2 Experimental results

The experiment was performed with a 48-pole SPM motor to demonstrate the performance of the proposed algorithm. Fig. 10 shows the experimental setup. The switching devices IGBTs were switched on and off at the frequency of 10 kHz for controlling the PM motor. The proposed algorithm was implemented with a TM320F28335 digital signal processor using the C-language.

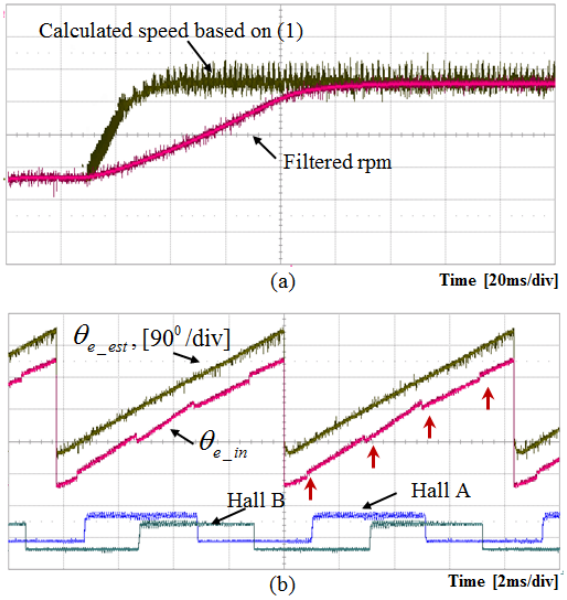

Fig. 12. Experimental results conducted with k=100 and f_c=80 Hz

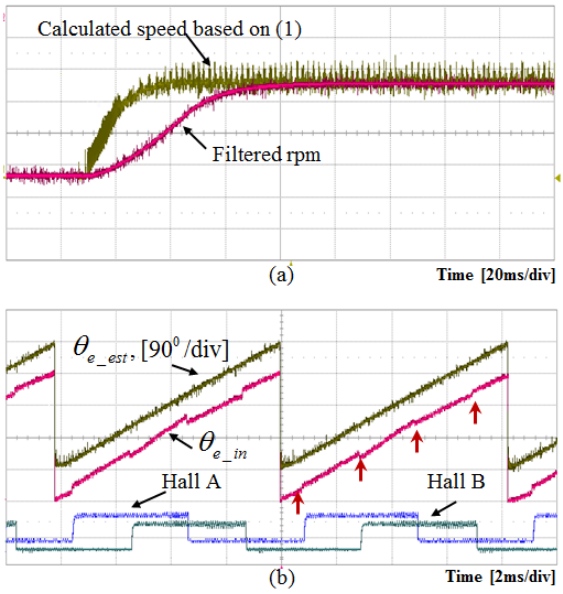

Fig. 13. Experimental results conducted with k=100 and f_c=250 Hz

Fig. 11 illustrates the experimental results (a) without and (b) with the proposed bump-removal scheme carried out at 300 rpm rotation, separately. The gain k and cutoff-frequency f_c were chosen as 150 and 100 Hz, respectively, which are different from values used in the simulations, in order to show the robust performance of the proposed scheme for other values of k and f_c. Fig. 11(a) clearly depicts the bumps in the position signal generated whenever the Hall event occurs and the distorted motor current. In contrast, Fig. 11(b) displays that the bump-less position signal and the resultant sinusoidal phase current, which clearly illustrates that the proposed method, having the brief structure, can get the linearly changing rotor position without angle deviation.

Figs. 12 and 13 show the experimental results corresponding to the simulation waveforms of Figs. 7 and 8, respectively, in which f_c is set as 80 Hz and 250 Hz, separately. The rpm of the motor based on (1) and the filtered (denoted as estimated) motor speed are displayed in the upper figure at the operation of 300 rpm. θ_{e_in}, θ_{e_est}, and Hall A & B waveforms are illustrated in the lower figure.

Depending on the filtering frequency f_c, the convergence speed of the filtered motor rpm varies, but as shown in each diagram of Fig. 13(b), the detection of the bumpless position signal without any angular discrepancy is achieved by the proposed scheme, regardless of f_c value.

5. Conclusion

This paper proposed a new scheme to eliminate the bumps in the position signal using binary-type Hall sensors. The proposed method featured a very simple structure consisting of the first order low-pass filter and the first order observer. The estimated position signal by the proposed method has no phase delay compared to the signals calculated by Hall sensor events. The paper explained the reason why the phase delay does not occur. The proposed bump-removal scheme did not use any of the electrical or mechanical constants such as inertia and flux-linkage. In addition, the proposed algorithm has eliminated the necessity of motor torque calculation and additional processing for the detection of system parameters. Through simulations and experiments, the improvement of the control performance and the adequacy of the proposed method have been verified.

Acknowledgements

This research was supported by Basic Science Research Program through the National Research Foundation of Korea(NRF) funded by the Ministry of Science, ICT and Future Planning(NRF- 2016R1A2B4011954).

References

[1] H. J. Ahn and D.M. Lee, "A new bumpless rotor-flux position estimation scheme for vector-controlled washing machine," *IEEE Trans. on Indus. Informatics*, vol. 12, no. 2, pp. 466-473, April 2016.

[2] C. H. Hong, J. Lee, and D.M. Lee, "Sensorless scheme of interior permanent magnet synchronous motor with wide speed control range," *Journal of Power Elect.*, vol. 16, no. 6, pp. 2173-2181, Nov.

2016.
[3] S. Y. Jung and K.H. Nam, "PMSM control based on edge-field hall sensor signals through ANF-PLL processing," *IEEE Trans. Ind. Elect.*, vol. 58, no. 11, pp. 5121-5129, Nov. 2011.
[4] H. Kim, S. Yi, and R.D. Lorenz, "Using low resolution position sensors in bumpless position/speed estimation methods for low cost PMSM drives," *Industry Appli. Conf.,* Hong Kong, China, vol. 4, pp. 2518-2525, Oct. 2005.
[5] L. Kreindler, I. Iacob, G. Casaru, A. Sarca, R. Olteanu, and D. Matianu, "PMSM drive using digital hall position sensors for light EV applications," *Inter. Symp. on Advanced Topics in Electrical Eng.*, Bucharest, Romania, pp. 199-204, 2015.
[6] F. G. Capponi, G. Donato, L. Ferraro, O. Honorati, M.C. Harke, and R.D. Lorenz, "AC brushless drive with low-resolution Hall-effect sensors for surface-mounted PM Machines," *IEEE Trans. on Industry Appli.*, vol. 42, no. 2, pp. 526-535, Mar./Apr. 2006.
[7] S.B. Ozturk, B. Akin, H.A. Toliyat, and F. Ashrafzadeh, "Low-cost direct torque control of permanent magnet synchronous motor using Hall-effect sensors," *in Proc. Twenty-First Annual IEEE Applied Power Electronics Conf. and Expo.*, Dallas, USA, pp. 19-23, Mar. 2006.
[8] A. Lidozzi, L. Solero, F. Crescimbini, and A. Napoli, "SVM PMSM drive with low resolution hall effect sensors," *IEEE Trans. Power Electron.*, vol. 22, no. 1, pp. 282-290, Jan. 2007.
[9] P. B. Beccue, S. D. Pekarek, B. J. Deken, and A. C. Koenig, "Compensation for asymmetries and mis-alignment in a Hall-effect position observer used in PMSM torque-ripple control," *IEEE Trans. Ind. Appl.*, vol. 43, no. 2, pp. 560-570, Mar./Apr. 2007.
[10] T. D. Batzel and K. Y. Lee, "Slotless permanent magnet synchronous motor operation without a high resolution rotor angle sensor," *IEEE Trans. Energy Conv.*, vol. 15, no. 4, pp. 366-371, Dec. 2000.
[11] A. Yoo, S.K. Sul, D.C. Lee, and C.S. Jun, "Novel speed and rotor position estimation strategy using a dual observer for low-resolution position sensors," *IEEE Trans. Power Electron.*, vol. 24, no. 12, pp. 2897-2906, Dec. 2009.
[12] Z. M. Dalala, Y. H. Cho, and J. H. Lai, "Enhanced vector tracking observer for rotor position estimation for PMSM drives with low resolution Hall-effect position sensors," *IEEE Inter. Electric Machines & Drives Conf.*, pp. 484-491, 2013.
[13] J. H. Lee, C. H. Hwang, K. M. Kim, W. C. Lee, C. Y. Won, and Y.R. Kim, "Optimal washing time control algorithm for the drum washing machine using an inertia estimator," *in Proc. IEEE 2nd Inter. Power and Energy Conf.*, Johor Bahru, Malaysia, pp. 1393-1398, Dec. 2008.
[14] Y. J. Han, C. Y. Lee, and Y. Sun, "A study on the sensor applications for position detection and guideway monitoring in high speed Maglev," *Modern Mech. Engineering*, vol. 4, no. 4, pp. 165-174, 2014.

Dong-Myung Lee received his B.S. and M.S. in Electrical Engineering from Hanyang University, Seoul, Korea, in 1994 and 1996, respectively, and his Ph.D. in Electrical and Computer Engineering from the Georgia Institute of Technology, Atlanta, Georgia, USA, in 2004. From 1996 to 2000, he worked for LG Electronics Inc., Seoul, Korea. From 2004 to 2007, he was employed by the Samsung SDI R&D Center, Yongin, Korea, as a Senior Engineer. From 2007 to 2008, he was with the Department of Electrical Engineering, Hanyang University, as a Research Professor. Since 2008, he has been an Associate Professor with the School of Electronic and Electrical Engineering, Hongik University, Seoul, Korea. His current research interests include variable speed drives and power conversion scheme for renewable energy sources and energy storage systems.